ISSN 1996-3343

Asian Journal of Applied Sciences

http://knowledgiascientific.com

Knowledgia SCIENTIFIC
A Place to Publish Outstanding Research

Asian Journal of Applied Sciences 1 (2): 158-167, 2008
ISSN 1996-3343

Mineralogical and Fluid Inclusions Studies on the Mineralized Bostonite Dykes at UM Guruf Area, Central Eastern Desert, Egypt

B.H. Ali, M.G. El-Feky, M.A. Ali and E.K. Abu Zeid
Nuclear Materials Authority, P.O. Box 530, El-Maadi, Cairo, Egypt

Abstract: The present study aims to elucidate the mineralogical and petrographic composition of the dykes as well as their radioactivity and factors controlling uranium mineralizations. The detailed spectrometric survey on these bostonite dykes revealed their enrichment in U and Th (700 ppm eU and 48 ppm eTh, in average, respectively). The mineralogical studies on these dykes indicate the presence uranophane and kasolite as radioactive minerals. Zircon and fluorite are the main accessory minerals and they are barren from any radioelements. The presence of the radionuclides as secondary minerals, e.g., uranophane and kasolite and their absence in the uranium-bearing minerals such as zircon and fluorite suggest that the radioactivity of bostonite is not orthomagnetic but gained post-magmatically via hydrothermal solutions. Fluid inclusion studies on quartz reveal that the temperature of the mineralizing carbonic fluids was between 282 to 303°C and give salinity values ranging from 0 to 0.9 wt% NaCl equivalent and trapped under lithostatic pressure equals 65 bar. These rich CO_2-fluids caused remobilization of uranium from the magmatic zircon and fluorite in the form of uranyl-monocarbonate. Mixing of low temperature shallow meteoric aqueous fluid with hot carbonic fluids (~190°C) through fractures system and, consequently, the fluids pressure releasing to about 4.7 bar. The temperature gradient, changing pH and the fluid/rock interaction may have played active role during the post-magmatic stage that includes precipitation of secondary uranium as uranophane and kasolite.

Key words: Bostonite, mineralization, uranophane, kasolite and fluid inclusion

INTRODUCTION

According to El-Ramly and Hussein (1982), the crustal evolution of the Nubian Shield was enhanced by several subalkaline to alkaline rocks from the early Paleozoic until the Tertiary (570-700 Ma). These rocks include shallow ring complexes, trachyte sheets, dyke intrusions and Tertiary basalts. The dyke intrusions in Egypt, according to Stern and Hedge (1985), were distinguished into three main episodes as follows:

- Late Precambrian metamorphosed dykes: They were emplaced and metamorphosed under amphibolite and greenschist facies conditions.
- Late Precambrian unmetamorphosed dykes: Described by El-Ramly and Akaad (1960) as post-granite dykes. They post-date the folding and metamorphic events of the Egyptian basement complex. The post-granite dykes represent the Pan-African orogeny. They cut through all the Precambrian rocks and consist of variable rocks ranging from basaltic to rhyolitic types, including several generations of subalkaline and alkaline magmatic series.
- Neogene dykes that are of basic composition and mostly pertain to the early rifting stages of the Red Sea.

Corresponding Author: B.A. Ali, Nuclear Materials Authority, P.O. Box 530, El-Maadi, Cairo, Egypt

As far as the authors are aware, there is no previous detailed studies on the bostonite dykes of the study area, Um Guruf area. The present work aims to elucidate the mineralogical and petrographic composition of the dykes as well as their radioactivity and factors controlling uranium mineralizations. To verify this aim, the bostonite dykes have thoroughly been studied and sampled in the field. Detailed petrographic, radiometric, fluid inclusion studies and Scanning-Electron Microscope (SEM) examination were carried out on whole rock and picked grains as well.

MATERIALS AND METHODS

The study area is located at the central part of the Eastern Desert of Egypt between latitudes 25" 45' and 25" 50' N and longitudes 34" 00' and 34" 10' E (Fig. 1). It lies about 100 km SW Qussier town. The area is accessible from the Red Sea through Wadi El-Dabbah desert track. The rock types exposed in the study area, starting from the oldest are metavolcanics, older granitoids, biotite granites and alkali feldspar granites.

The metavolcanics (island arc volcanics) are the oldest rock units in the studied area (Fig. 1). They occur as belt exposed at the northern side of the studied area. They cover about 20% of total mapped area and are intruded by both older and younger granitoids (El-Sibai and Um Guruf granites, respectively). They are characterized by the presence of Banded Iron Formation (BIF) due North of wadi El-Dabbah (Fig. 1).

The older granitiods are the second dominant rock unit in the studied area and they cover about 10% of the mapped area. They represent the southern continuation of a large mass of batholithic dimension. These deformed rocks are generally characterized by their high relief. The older granitoids intrude the metavolcanics and enclose several xenoliths of different sizes and shapes. Basalt, dolerite and alkaline bostonite dykes follow the NW-SE, NE-SW and nearly E-W directions. NNE-SSW and N-S sets of faults intersect the granitic pluton. These faults are mainly of strike-slip type (sinistral) and vary in length from 1.5 to 4 km.

The biotite granite south Gabal Um Guruf volcanics forms an elongated belt trending NW-SE and extent for about 1.5 km long with 1 m width. It exhibits high relief (537 m a.s.l.). This granite is medium-to coarse-grained, massive, jointed and has equigranular texture. The colour ranges from pink to buff and has exfoliation, cavernous and bouldery appearance. It intrudes metavolcanics and sends several offshoots and contains several xenoliths of different shapes and sizes from older rocks. The

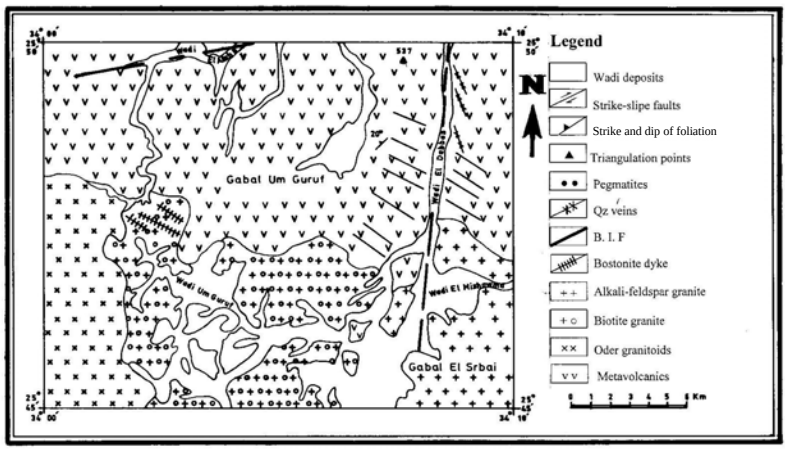

Fig. 1: Geological map of Um Guruf area, Central Eastern Desert, Egypt

NW-SE trending bostonite dykes bound the northwestern boundary biotite granites of Gabal Um Guruf area, where the granite becomes mylonitized cataclased especially at the contacts. The emplacement of younger granite was followed by the intrusion of the bostonite dykes These granites are characterized by the presence of pegmatite pockets composed of feldspars, quartz and mica. The pegmatites belong to both normal and zoned types. All rock units are dissected by numerous mafic and felsic dykes. Felsic dykes are of bostonitic composition, massive, fine-grained and pink to yellowish pink in colour. They show trachytic texture. The dykes extend in length from 0.5 to 1.5 km and from 0.5 to 1 m in width. These bostonite dykes possess sharp contact with their enclosing granitic rocks.. However, the dykes with a fine-grained, even fabric, are thought to be aplites.

RESULTS AND DISCUSSION

The studied rocks are mainly composed of potash-feldspars and iron oxides. The former occurs as euhedral crystals of medium grain size (from 1.5 to 2 mm length). They are completely altered to amorphous silica and clayey materials by the hydrothermal solutions and arranged in radiated or randomly oriented aggregates forming bostonitic texture (Fig. 2a). Iron oxides occur epigenetically as hematite staining the feldspars and as magnetite filling the fractures or as magmatic crystalline magnetite (black) crystals (Fig. 2b). The rocks are dominated by radioactive minerals such as uranophane and kasolite.

Uranophane

($CaH_2(SiO_4)_2UO_2.5H_2O$), is considered as one of the most important economic-secondary uranium deposits. It is a monoclinic uranyl silicate mineral fairly common in the oxidized zone of most deposits (Cesbron *et al*., 1993). The conditions required for the formation of secondary uranyl silicates have been investigated by many authors (e.g., Nininger, 1954; Frondel, 1956; Finch and Ewing, 1992; Korzeb *et al*., 1997). These conditions include both the late stages reactions of uraninite with hydrothermal solutions and also alteration by ground water. The occurrence of uranophane on rock surfaces in some Swedish secondary deposits was attributed to near-surface weathering and mobilization under ambient ground-water conditions (Lofvendahl and Holm, 1981). In the present study, uranophane occurs as massive mineralization with platy and granular forms and show dull, greasy and/or waxy luster. Its colour ranges from canary yellow to lemon but pale yellow is also common. Yellow spherulitic aggregates and needles filling the spaces and fractures of potash feldspars are the most common forms of uranophane (Fig. 2c, d). Cryptocrystalline strips adsorbed by the iron oxides are also present.

Kasolite

It is the only uranyl-silicate with major lead ($Pb(UO_2)(SiO_4).H_2O$). It is a secondary mineral and occurs as a product of reaction of meteoric water carrying silica with earlier formed secondary uranium minerals. Rismasite (1982) notes that uranium released during the alteration of pitchblende in the oxidation zone forms several generations of secondary uranium minerals, the earlier ones being enriched in lead, e.g., kasolite and masuyite, where the later is impoverished in lead. Under the microscope, kasolite is characterized by its reddish orange shade and it occurs as euhedral crystal of prismatic form (Fig. 2c, d) or as encrustation (Fig. 2e).

Generally, Kasolite occurs as aggregates, sometimes stained by iron oxy-hydroxides. Kasolite is, occasionally, found as inclusions in feldspar. This causes radiation damage to feldspar lattice (Fig. 2e). Opaque haloes surround such kasolite grains contain significant amounts of iron and uranium. Such haloes act as pathways to hydrothermal solutions that cause alteration of kasolite which appears almost barren from uranium and mainly composed of lead (Table 1). The presence of kasolite has been confirmed by the SEM examination and XRD analysis (Fig. 3a and Table 1, 2).

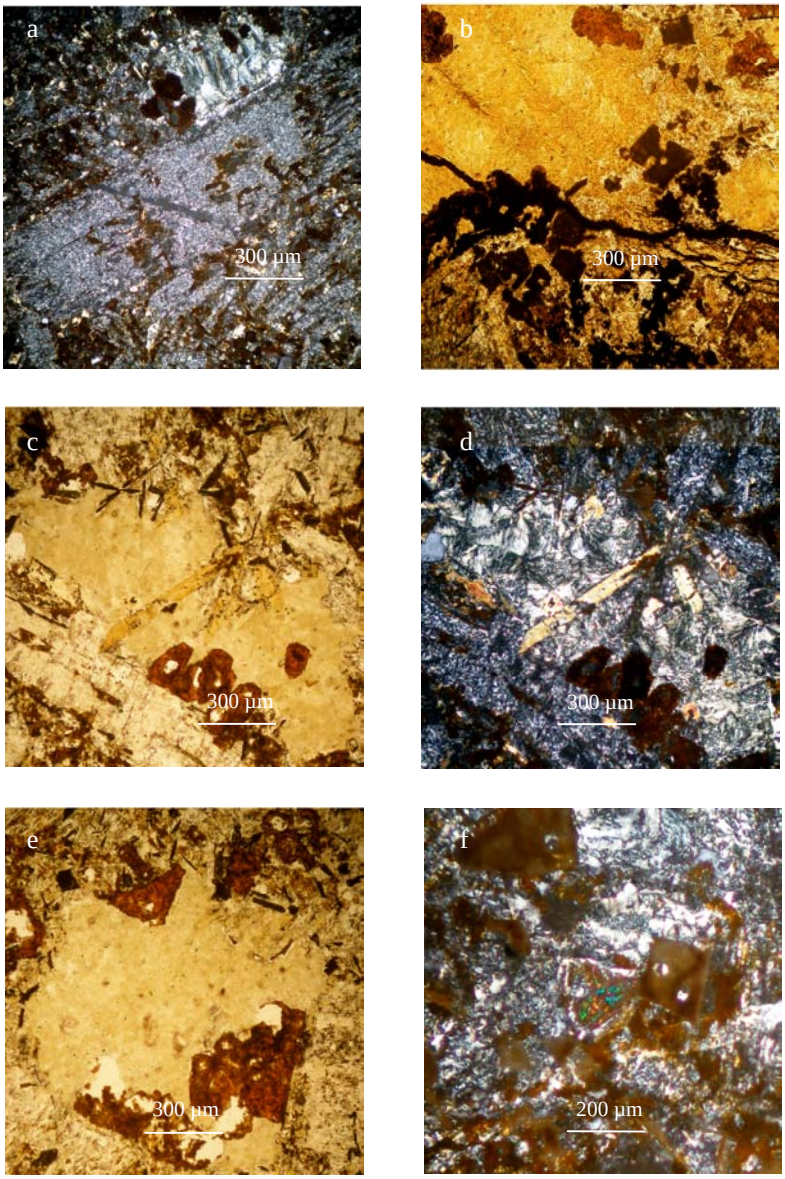

Fig. 2: Photomicrographs of bostonite showing: (a) Euhedral crystal of potash feldspar altered to clays and amorphous silica, CN, (b) A fracture in uranophane filled with iron oxides and associated with euhedral crystals of magnetite, PPL, (c) Euhedral monoclinic crystals of Kasolite associating uranophane, PPL, (d) The same view showing that uranophane occurs as needles and spherulitic aggregates, associating uranophane. CN, (e) Encrustations of kasolite associating uranophane, PPL and (f) Euhedral crystal of zircon showing its characteristic interference colors and overgrowth associating euhedral crystals of kasolite

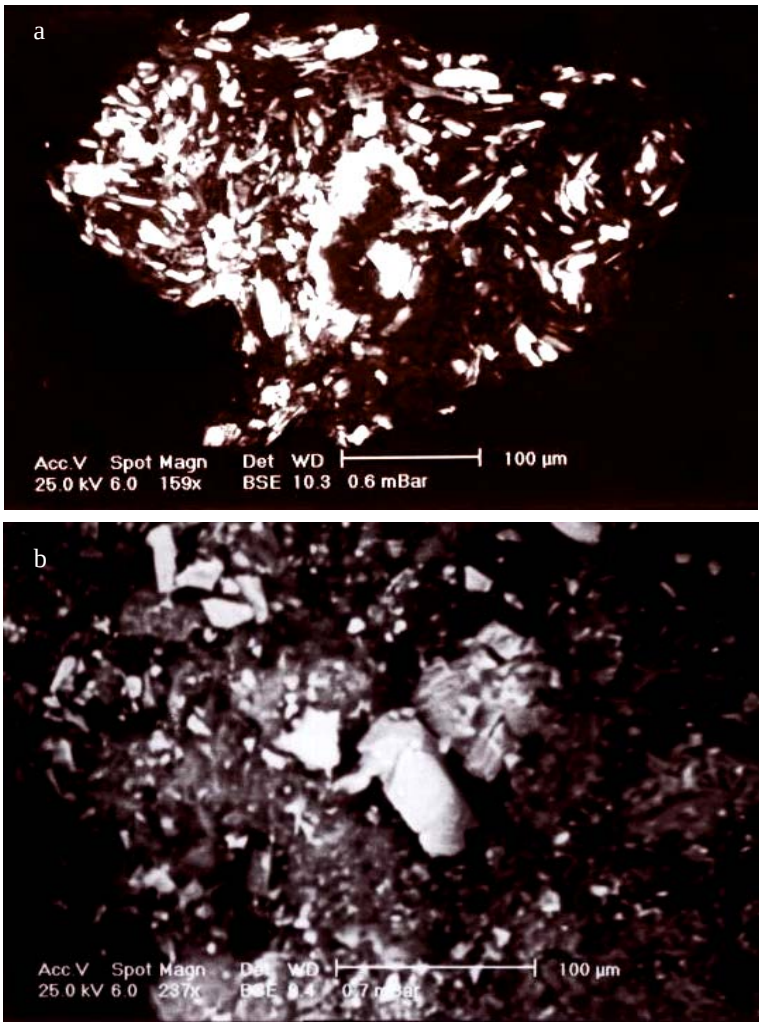

Fig. 3: (a) Analyzed grains of kasolite and (b) Analyzed grains of fluorite

Table 1: EDX analysis data of kasolite

Elements (%)	Spot No. 1	Spot No. 2	Spot No. 3	Spot No. 4
Al	4.96	26.99	2.97	5.04
Si	7.31	33.84	1.60	13.35
K	3.09	1.01	<0.50	1.08
Ti	<0.50	0.88	<0.50	1.03
Mn	<0.50	<0.50	44.56	30.44
Cu	<0.50	<0.50	1.51	1.63
Zn	<0.50	<0.50	2.27	4.88
Ce	0.76	1.43	<0.50	<0.50
Fe	1.58	4.88	3.27	12.44
Y	<0.50	<0.50	<0.50	4.72
Pb	35.57	15.87	42.06	24.32
U	46.44	15.10	0.85	1.09

*The data are qualitative since oxygen, carbon and hydrogen are not analyzed for their low precision

Table 2: X-ray diffraction analysis data of kasolite

Data of sample No. 3		ASTM data of kasolite	
d spacing (Å)	I/I°	s spacing (Å)	I/I°
6.5	23	6.61	60
6.08	12	6.19	20
5.26	11	5.31	40
4.72	4	4.76	20
4.19	34	4.19	80
3.53	44	3.53	70
3.34	12	3.38	10
3.26	100	3.36	100
3.06	35	3.07	50
2.91	41	3.93	90
2.73	6	2.73	30
2.63	5	2.64	30
2.46	7	2.47	30
2.41	7	2.42	20
2.36	6	2.37	20
2.17	23	2.18	30
2.12	9	2.11	20
2.04	7	2.05	30
1.97	16	1.96	50
1.92	6	1.91	10
1.87	10	1.87	20
1.74	11	1.74	40
1.67	13	1.67	50
1.46	7	1.45	30

Zircon is a rare and occurring as euhedral crystals displaying regular optical properties, referring to its depletion in radioelements (Fig. 2f). The examination of fluorite by SEM indicates its poverty in radioelements, but it is enriched in Fe, K, Si and Al with Ca and F (Fig. 3b).

Radiochemically, the average concentration of eU, eTh, Ra and K of the bostonite samples are measured to be 700, 48, 662 ppm and 3.22%, respectively. Uranophane can't be determined using SEM or XRD being closely associated with kasolite, which is widely distributed within the studied bostonites. However, kasolite can be considered as the major contributors to the total uranium in bostonite, where U ranges from 15 to 46% (Table 2). Similar observation has also been recorded for other localities by El-Galy (1998), Ali *et al*. (2005) and Abdel Warith *et al*. (2007). In addition to uranium, kasolite is also characterized by the presence of Si, Al, K, Fe, Pb, Ti, V, Cu, Mn, Zn and Ce in variable concentrations (Table 2).

FLUID INCLUSION STUDIES

The main objectives of this study are to determine the composition, temperature, salinity and pressure of the U-mineralizing fluid in the bostonite under consideration. One hundred and fifty measurements were obtained. Doubly polished thin sections 10 to 100 μm thick were used for detailed petrographic study and microthermometric analysis. The measurements were conducted with USGS gas flow heating/freezing stage at Applied Geology Department of Curtin University for Technology in Australia. Freezing measurements on the fluid inclusion were made before any heating because of possible deformation and decrepitating of inclusions at high temperatures, CO_2 rich inclusions commonly decrepitated before final homogenization. All fluids homogenized to liquid state. The data were processed using Bulk Program after Baker (2003).

Petrography and Types of Fluid Inclusions

Most of large fluid inclusion in quartz crystals range in size from 5 to 25 μm. They have well defined regular boundaries but some notably larger and quiet irregular which characterize liquid-vapor

aqueous fluid inclusion. The smallest fluid inclusions (1 to 15 μm) are included in fluorite crystals. On based of number of inclusions and their nature and proportion of phases (at room temperature) they can be classified into 3 types:

- Mono-phase fluid inclusions that consist of either liquid (L) or vapor (V). They are small (≤ 5 μm) in size, spherical in shape and were not adequate for precise measurements. The vapor fluid inclusions (V) usually coexist with vapor liquid (VL) one which may indicate boiling fluids.
- Aqueous fluids (LV) with $H_2O_{(L)}+H_2O_{(v)}$ composition. They are primary inclusions common in quartz crystals with liquid ratio ≥ 75%.
- CO_2 rich fluids (VL). They consist of $H_2O_L+CO_{2L}+CO_{2V}$, sometimes they form one gaseous phase. Most of these inclusions are secondary and pseudo-secondary in origin. They are common in fluorite crystals. Some fluids are decrepitated due to overheating by later hydrothermal fluids. The primary large fluids are sometimes surrounded by mono-phase smaller inclusions.

Microthermometry

Fluid inclusions were frozen by super cooling to temperature between -70 and -90°C. The frozen inclusion were then heated 1-2°C min^{-1} and the melting temperatures of the solid phases formed during freezing were recorded. The final melting temperature of ice was recorded within 0.1°C and was reproduced within ±0.2°C. It enables collections of fluid inclusion salinities and hence parent liquor salinities using the equation of Bodnar, (1993), in Bulk computer program (Baker, 2003). In carbonic fluids, CO_2 gas appears at slightly below room temperature and display a strong marked freezing at -95.5°C. Heating runs were carried out with heating rates of 6°C min^{-1} until homogenization was considered to be approached. Homogenization temperature was determined as the mean of the highest temperature where a gas bubble was present and the lowest temperature where a gas bubble did not observe. All inclusions in the studied samples homogenized to a liquid phase. Reproduce ability of the measurements is approximately ±1°C. Thermocouple accuracy was ±0.1°C over the investigated interval 0 to -40°C.

Low Temperature Phase Changes

Inclusions were typically frozen to about -110°C. The temperature of initial melting (Ti) and final melting (Tm) of ice were measured in some LV inclusions but it is difficult to be measured in the smallest one. In (LV) fluid inclusions Ti values range from -29.9 to -49.5°C indicating H_2O+NaCl + KCl±CaO and MgO system (Davis *et al*., 1990). Final melting temperatures of ice (Tm) rang from -8.3 to -21.2°C corresponding to salinities of 12.29 to 23.75 wt% NaCl equation, respectively (Table 3, Fig. 4a) (Bodnar, 1993). In CO_2 rich inclusions, CO_2 gas appears at or slightly below room

Table 3: Microthermometric data for aqueous fluid inclusions

Frequency	Th°C	Ti°C	Tm°C	NaCl equation	P (bar)
10	151.1	-45.0	-19.4	22.56	4.97
9	140.6	-41.0	-18.6	21.99	4.58
10	156.4	-49.1	-14.2	18.44	5.30
8	144.2	-36.5	-13.9	18.16	4.08
12	185.5	-49.5	-8.3	12.29	9.12
7	161.9	-46.7	-21.2	23.75	5.75
10	189.9	-45.5	-18.4	21.85	7.86
11	178.6	-32.2	-13.1	17.42	10.10
5	190.1	--29.9	-17.9	21.48	9.66
8	188.1	-37.6	-18.2	21.70	8.53
13	182.4	-42.1	-17.4	21.10	6.32
11	167.5	-48.4	-20.5	22.86	6.32
10	169.4	-47.2	-18.2	21.70	6.55
14	191.2	-39.1	-17.4	20.59	10.35
12	159.7	-44.1	-16.9	20.71	6.56

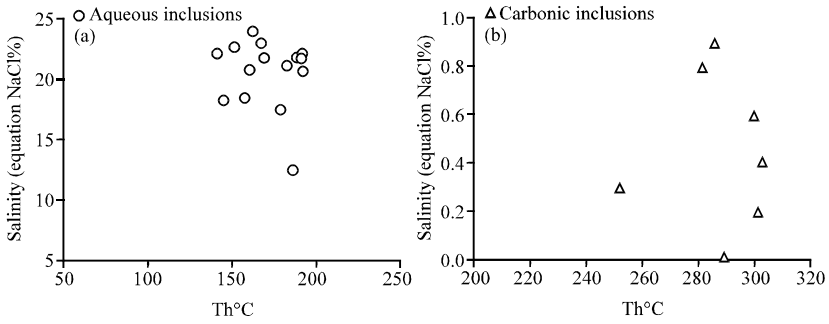

Fig. 4: Homogenization temperature (Th°C) vs. salinity (wt% NaCl equ.) in: (a): aqueous inclusions, (b): carbonic inclusions

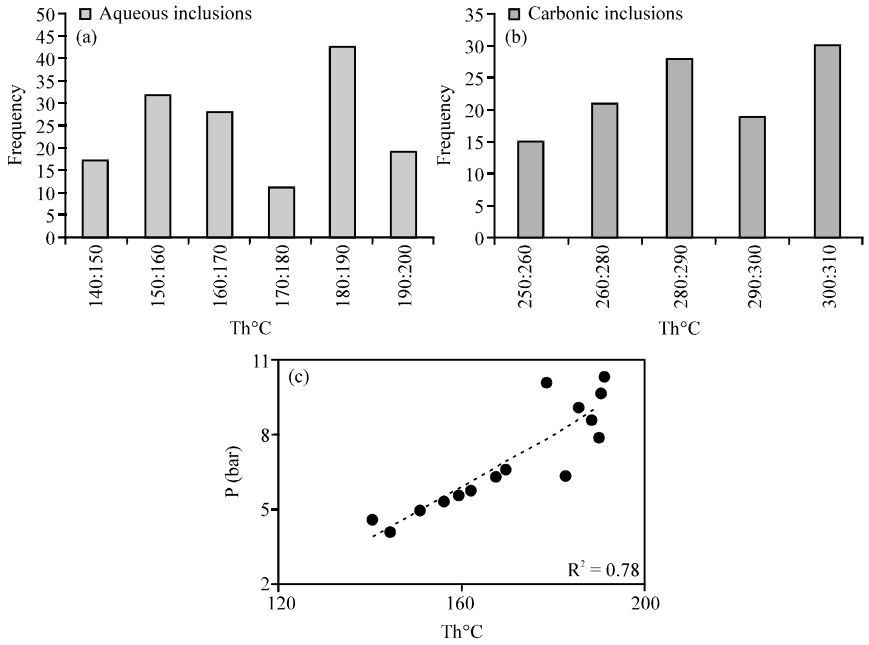

Fig. 5: Histogram for homogenization temperature (Th°C) in: (a): Histogram for homogenization temperature (Th°C) in aqueous inclusions (b): Histogram for homogenization temperature (Th°C) in carbonic inclusions and (c)- Homogenization temperature (Th°C) vs. pressure (bar) in aqueous inclusions.

temperature. The triple- point temperature (Tm CO_2) range -56.6 and -54.9°C which give no indication for other gases than CO_2, where Tm CO_2 values below -56.6°C indicate the presence of other gases (CH_4±N_2, Burruss, 1981; Johnson and Hollister, 1995). CO_2 rich inclusion displayed a strong marked freezing at -96.5°C. Clathrate (Tm cl) formation in such inclusions was detected in visible CO_2 liquid indicates that they contain appreciable amount of CO_2. It is ranging from 9.3 to 10.0°C, which confirm absence of other gases. Depending on this temperature, salinity for these inclusions was determined using Chen equation (1972) which confirmed by Darling (1991). It is ranging from 0 to 0.9 wt% NaCl equation (Table 4, Fig. 4b).

Table 4: Microthermometric data for carbonic fluid inclusions

Frequency	Th°C total	Th°C CO_2	Th m° CO_2	Th m°C calthrate	NaCl equation	P (bar)
15	289.6	22.6	-56.2	10.0	0.0	60.86
10	301.9	23.8	-56.3	9.9	0.2	62.58
20	303.1	26.4	-56.5	9.8	0.4	66.48
15	252.3	26.3	-54.9	9.9	0.3	66.28
21	281.9	25.1	-56.6	9.4	0.8	64.48
19	300.1	24.8	-55.4	9.7	0.6	64.03
13	285.9	25.7	-56.2	9.3	0.9	65.38

High Temperature Changes

Both aqueous and carbonic fluid inclusions homogenized to liquid state. In aqueous fluids (LV), the homogenization temperature (Th) is ranging from 140.6 to 191.2°C with obvious mode from 180 to 190°C (Fig. 5a). The total homogenization of CO_2 rich inclusions range from 281.9 to 303.1°C with familiar frequency at (300: 310°C), (Fig. 5b) while Th for CO_2 liquid and gas, range from 22.6 to 26.4°C, which indicate to pure H_2O+CO_2. The strong positive correlation (R^2 = 0.78) between homogenization temperature (Th) and the static pressure (P) is evidence that pressure release had play an active part during post-magmatic stage of uranium mineralizations (Fig. 5c).

CONCLUSIONS

Kasolite and uranophane occur mainly as fracture and spaces filling indicating the role of hydrothermal solutions in uranium mineralization. Presence of the radioelements in the form of secondary radioactive minerals such as uranophane and kasolite and their absence in the uranium-bearing minerals such as zircon and fluorite suggest that the radioactivity of bostonite is not proper but it is gained by the post-magmatic processes and hydrothermal solutions. Also, the appearance of altered kasolite members nearly barren from uranium and mainly composed of radiogenic lead may be considered as evidence that there is more than one episode of hydrothermal alteration. The first stage leads to uranophane and kasolite mineralization where the second ones were accompanied by their alterations.

The mineralizing fluids with temperature (282 to 301°C), were CO_2 rich, suggesting that uranium was transported mainly in the form of uranyl-monocarbonate complex (UO_2 CO_3) by low saline fluids (range from 0.0 to 0.9 wt% NaCl equation) and under high pressure (range from 57.28 to 66.58 bar). Secondary uranium mineralization could have result from CO_2 effervescence from the mineralized fluids as a result of pressure release to about 4.68 bar and consequent dissociation of the uranyl-monocarbonate, (Min and Kasumura, 1997). Other factors that may have played a part are: the temperature gradient away from the heat source (it reaches to about 140°C), the fluid/rock interaction and mixing of the hydrothermal fluids with shallow meteoric water in related fracture system during post magmatic stage. All these factors lead to change in pH value and consequently precipitation of secondary uranium mineralizations, in the form of uranophane, kasolite.

REFERENCES

Abdel Warith, A., M.F. Raslan and M.A. Ali, 2007. Mineralogy and radioactivity of pegmatite bodies from the granitic pluton of Gabal Um Tager El-Tahtani area, Central Eastern Desert, Egypt. The 10th International Mining, Petroleum, and Metallurgical Engineering Conference, March 6-8 2007, Mining, Code No. M3, pp: 101-113.

Ali, M.A., M.F. Raslan and M.G. El-Feky, 2005. Radioactivity and mineralogy of some pegmatite bodies from Gabal Al-Farayid granites, South Eastern Desert, Egypt. The 9th International Mining, Petroleum, and Metallurgical Engineering Conference, February 21-24, 2005, Mining Code No. M 1, pp: 47-57.

Baker, J.R., 2003. FLUIDS, package of computer programs for fluid inclusion studies Program 1: BULK, version 01/03.

Bodnar, R.J., 1993. Revised equation and stable for determining the freezing point depression of H_2O-NaCl solutions. Geochim. Cosmochim. Acta, 57: 683-684.

Burruss, R.C., 1981. Equilibria at constant volume. Am. J. Sci., 281: 1104-1126.

Cesbron, F., P. Ildefonse and M.C. Sichere, 1993. New mineralogical data on uranophane and β-uranophane: Synthesis of uranophane. Mineral. Mag., 57: 301-308.

Chen, H.S., 1972. The properties of carbon dioxide hydrate. Office of Saline Water, Research and Development Progress Report No. 830, pp: 1-55.

Darling, R.S., 1991. An extended equation to calculate NaCl contents from final clathrate melting temperatures in H_2O-CO_2-NaCl fluid inclusions: Implications for P-T isochore location. Geochim. Cosmochim. Acta, 55: 3869-3871.

Davis, D.W., T.K. Lowenstein and R.J. Spencer, 1990. Melting behavior of fluid inclusions in laboratory-grown halite crystals in the systems NaCl-H_2O, NaCl-$MgCl_2$-H_2O and NaCl-$CaCl_2$-H_2O. Geochim. Cosmochim. Acta, 54: 591-601.

El-Galy, M.M., 1998.. Geology, radioactivity, geochemistry and tectonic setting of selected granitic rocks, West Gulf. Ph.D Thesis, Tanta University, Egypt.

El-Ramly, M.F. and M.K. Akaad, 1960. The basement complex in the central Eastern Desert of Egypt between lat. 24° 30' and 25° 40'. Geol. Surv. Egypt, 5: 15-15.

El-Ramly, M.F. and A.N. Hussein, 1982. The alkaline ring complex of Egypt. Geol. Surv. Egypt, 63: 16-16.

Finch, R.J. and R.C. Ewing, 1992. The corrosion of uraninite under oxidizing conditions. J. Nucl. Mater., 190: 133-156.

Frondel, C., 1958. Systematic mineralogy of uranium and thorium. U.S. Geol. Survey Bull., 1064: 400-400.

Johnson, E.L. and L.S. Hollister, 1995. Syndeformational fluid trapping in quartz: Determining the pressure-temperature conditions of deformation from fluid inclusions and formation of pure CO_2 fluid inclusions during grain-boundary migration. J. Metamorphic Geol., 13: 239-249.

Korzeb, S.L., E.E. Foord and F.E. Lichte, 1997. The chemical evolution and paragenesis of uranium minerals from the Ruggles and Palermao granitic pegmatites, New Hampshire. Can. Mineralogist, 35: 135-144.

Lofvendahl, R. and E. Holm, 1981. Radioactive disequilibria and apparent ages of secondary uranium minerals from Sweden. Lithos, 14: 189-201.

Nininger, R.D., 1954. Minerals for Atomic Energy: A Guide to Exploration for Uranium, Thorium and Beryllium. 1st Edn. D. Van Nostrand Company Inc., Toronto, pp: 259.

Raslan, M.F., 1996. Mineralogical and beneficiation studies for some radioactive granites along Wadi Balih, North Eastern Desert, Egypt. M.Sc. Thesis, Cairo University,

Rismasite, J., 1982. The leaching of radionuclides and other ions during alteration and replacement of accessory minerals in radioactive rocks. Paper Geol. Surv. Can., 82-iB: 253-253.

Stern, R.J. and C.E. Hedge, 1985. Geochronologic and isotopic constraints on late precambrian crustal evolution in the Eastern Desert of Egypt. Am. J. Sci., 285: 97-127.